

# Ultralow-loss and temperature-stable self-composite microwave dielectric ceramic of $\text{Li}_4\text{MgSn}_2\text{O}_7$ – $\text{Li}_2\text{Mg}_3\text{SnO}_6$ for LTCC applications

Shuang Zhang, Ruzhong Zuo \*

Institute of Electro Ceramics & Devices, School of Materials Science and Engineering, Hefei University of Technology, Hefei, 230009, PR China



## ARTICLE INFO

### Article history:

Received 16 January 2020

Received in revised form

16 March 2020

Accepted 24 March 2020

Available online 2 April 2020

### Keywords:

Li-based microwave dielectrics

Self-composite

Phase decomposition

LTCC

## ABSTRACT

A self-composite ceramic of  $\text{Li}_4\text{MgSn}_2\text{O}_7$  ( $\text{L}_4\text{MS}$ ) and  $\text{Li}_2\text{Mg}_3\text{SnO}_6$  ( $\text{L}_2\text{MS}$ ) phases with compositions  $\text{Li}_{2/3(1-x)}\text{Sn}_{1/3(1-x)}\text{Mg}_x\text{O}$  ( $x = 1/6$ )–y wt.%LiF was prepared for the first time by a conventional solid-state reaction method. The XRD results indicate that  $\text{L}_4\text{MS}$  and  $\text{L}_2\text{MS}$  ( $(\text{MgO})_{ss}$ ) phases can stably coexist only as sintering temperature is below 1200 °C, and their relative contents can be regulated by changing sintering temperature. The sintering aid LiF was used to not only reduce sintering temperature to suppress the  $\text{L}_4\text{MS}$  decomposition, but also obtain the dense ceramic body. Excellent microwave dielectric properties of  $\epsilon_r = 13.4$ ,  $\text{Q}_{xf} = 123,440$  GHz and near-zero  $\tau_f \sim -4.3$  ppm/°C were obtained in the  $y = 5$  sample sintered at 1000 °C for 6 h. For LTCC applications, both good chemical compatibility with Ag and optimum microwave dielectric properties of  $\epsilon_r = 13.0$ ,  $\text{Q}_{xf} = 78,180$  GHz and  $\tau_f = -9$  ppm/°C were achieved in the sample with  $y = 6$  as sintered at 850 °C, showing great application potentials in future microwave devices.

© 2020 Elsevier B.V. All rights reserved.

## 1. Introduction

The demand for low temperature co-fired ceramics (LTCC) materials has gradually increased with the rapid development of LTCC technology for miniaturization and integration of microwave devices. For LTCC applications, microwave dielectric materials should have a low sintering temperature and a super chemical compatibility with Ag electrode, in addition to appropriate dielectric constant  $\epsilon_r$ , high quality factor  $\text{Q}_{xf}$  and a near-zero  $\tau_f$  [1–3]. For this purpose, LTCC materials with excellent dielectric properties have been widely investigated so far [4–9].

Materials with rock-salt structures have attracted extensive attention in recent years for their ultra-low loss.  $\text{L}_2\text{Mg}_3\text{BO}_6$  ( $\text{L}_2\text{MB}$ , B = Ti, Sn, Zr) ceramics possess excellent microwave dielectric properties of  $\epsilon_r = 15.2$ , 8.8 and 12.6,  $\text{Q}_{xf} = 152,000$  GHz, 123,000 GHz and 86,000 GHz, and  $\tau_f = -39$  ppm/°C, -32 ppm/°C and -36 ppm/°C, respectively [10]. However, large negative  $\tau_f$  values have limited their practical applications. A near-zero  $\tau_f$  value was reported in  $\text{L}_2\text{MB}$  ceramics with the addition of  $\text{SrTiO}_3$  or  $\text{Ba}_3(\text{VO}_4)_2$  through forming secondary phases with an opposite-sign  $\tau_f$  value [11,12]. In addition, the porous microstructure

caused by lithium evaporation at higher sintering temperature have significantly deteriorated their microwave dielectric properties. Some efforts have been made to suppress the lithium volatilization in materials containing lithium by means of Li-rich atmosphere protection and adding sintering aids [13–20]. An ultrahigh  $\text{Q}_{xf}$  value of ~230,000–330,000 GHz was reported in LiF aided  $\text{Li}_2\text{Mg}_3\text{SnO}_6$  ( $\text{L}_2\text{MS}$ ) ceramics [15]. Recently, a new pure-phase  $\text{L}_4\text{MgSn}_2\text{O}_7$  ( $\text{L}_4\text{MS}$ ) with a positive  $\tau_f \sim 12.4$  ppm/°C was successfully synthesized by optimized calcination temperature and time [21], however it can stably exist as sintering temperature is below 1200 °C where unfortunately the sample can be poorly densified. The  $\text{L}_4\text{MS}$  ceramic doped with less than 3 wt% LiF was reported to exhibit  $\epsilon_r \sim 13.7$ ,  $\text{Q}_{xf} \sim 97,000$  GHz and  $\tau_f \sim -8$ –13 ppm/°C as sintered at 850 °C.

The phase diagram of the  $\text{Li}_{2/3(1-x)}\text{Sn}_{1/3(1-x)}\text{Mg}_x\text{O}$  system was proposed by M. Castellanos and A. R. West in early 1984 [22]. It is indicated from the phase diagram that there is a wide two-phase zone of  $\text{L}_4\text{MS}$  and  $\text{L}_2\text{MS}$  ( $(\text{MgO})_{ss}$ ) in the composition range of  $x = 1/7$ –9/10, in which the relative content of two phases clearly varies with composition and sintering temperature. In this work, a specially designed composition with  $x = 1/6$  was investigated for the purpose to achieve a new LTCC ceramic with excellent dielectric properties and particularly a near-zero  $\tau_f$  by self-compositing  $\text{L}_4\text{MS}$  and  $\text{L}_2\text{MS}$  phases, which means that the synthesized matrix is directly composed of two phases with opposite-sign  $\tau_f$  directly,

\* Corresponding author.

E-mail address: [\(R. Zuo\)](mailto:piezolab@hfut.edu.cn).

instead of the addition of a second phase. The phase content was controlled by adjusting appropriate sintering temperature via changing the concentration of sintering aid LiF. The phase evolution, microstructure, microwave dielectric properties of the  $x = 1/6$  sample and its chemical compatibility with Ag were studied in detail.

## 2. Experimental

The  $\text{Li}_{2/3(1-x)}\text{Sn}_{1/3(1-x)}\text{Mg}_x\text{O}$  ( $x = 1/6$ , abbreviated as  $\text{LSM}_{1/6}\text{O}$ ) ceramics were synthesized by a traditional solid-state reaction method using high-purity powders of  $\text{MgO}$ ,  $\text{SnO}_2$  and  $\text{Li}_2\text{CO}_3$  (Sinopharm Chemical Reagent Co. Ltd., Shanghai, China) as starting materials. Stoichiometric amounts of the powders were weighed according to the chemical formula, and were ball-milled for 4 h using zirconia balls and alcohol as the medium on a planetary milling machine. The resulting slurries were then rapidly dried and calcined at  $1000^\circ\text{C}$  for 22 h in air. The calcined powders were remilled for 6 h and then mixed together with 7 wt% PVA as a binder. The granulated powders were subsequently pressed into cylinders with dimensions of 10 mm in diameter and 5–7 mm in height. The specimens were first heated at  $550^\circ\text{C}$  in air for 4 h to remove the organic binder, and then sintered at  $1100^\circ\text{C}$ – $1250^\circ\text{C}$  for 6 h. Moreover, for LTCC applications and adjustment of the phase content,  $y$  wt.% LiF sintering aid ( $y = 3$ – $10$ ) was added into the as-calcined powder. After compaction, these samples were then sintered in air at  $800^\circ\text{C}$ – $1050^\circ\text{C}$  for 6 h at a heating rate of  $5^\circ\text{C}/\text{min}$ , and at a cooling rate of  $10^\circ\text{C}/\text{min}$ . To suppress the lithium evaporation, pellets were buried in the powder of the same composition.

The crystal structure of the fired ceramics was identified via an X-ray diffractometer (XRD, D/Max 2500 V, Rigaku, Japan) using  $\text{Cu K}\alpha$  radiation. The apparent densities of the sintered ceramics were measured by the Archimedes method. The microstructure of the pellets was observed by using a field-emission scanning electron microscope (FE-SEM; SU8020, JEOL, Tokyo, Japan). For the observation of grain morphology, the samples were polished and then thermally etched at a proper temperature for 15 min. Microwave dielectric properties of the ceramic cylinders were measured using a network analyzer (N5230C, Agilent, Palo Alto, CA) and a temperature chamber (GDW-100, Saiweisi, Changzhou, China). The  $\tau_f$  values of the samples were measured in the temperature range from  $20^\circ\text{C}$  to  $80^\circ\text{C}$  and calculated by the following equation:

$$\tau_f = \left( \frac{(f_2 - f_1)}{(T_2 - T_1)f_1} \right)$$

where  $f_1$  and  $f_2$  represent the resonant frequencies at  $T_1$  and  $T_2$ , respectively.

## 3. Results and discussion

**Fig. 1** shows the microwave dielectric properties, apparent density and XRD patterns of  $\text{LSM}_{1/6}\text{O}$  ceramics sintered at different temperatures for 6 h. It can be seen from **Fig. 1(a)** that  $\tau_f$  values tend to be near zero with decreasing sintering temperature. The  $Q_{xf}$  values, apparent density and  $\epsilon_r$  increase gradually with increasing temperature from  $1100^\circ\text{C}$  to  $1250^\circ\text{C}$ . The variation of microwave dielectric properties with changing sintering temperature can be well understood according to the sample density and the phase evolution. The increase of sample density with sintering temperature will generally help improve  $\epsilon_r$  and  $Q_{xf}$  values. However,  $\text{L}_4\text{MS}$  and  $\text{L}_2\text{MS}(\text{MgO})_{ss}$  phases can stably coexist only at a lower sintering temperature than  $1200^\circ\text{C}$  by comparing XRD patterns with standard patterns (JCPDS #37-1164 and JCPDS #39-

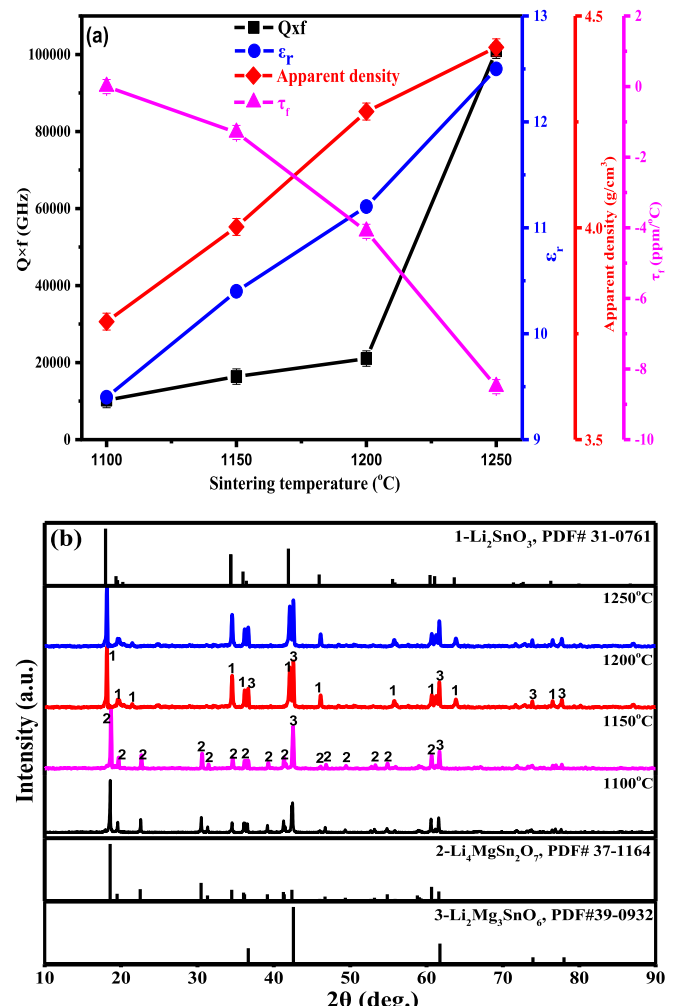


**Fig. 1.** (a) Microwave dielectric properties and apparent density and (b) XRD patterns of  $\text{LSM}_{1/6}\text{O}$  ceramics sintered at different temperatures for 6 h.

0932), as shown in **Fig. 1(b)**. Moreover, the content of  $\text{L}_2\text{MS}(\text{MgO})_{ss}$  phase was found to slightly increase with increasing temperature, keeping consistency with the phase diagram [20], which leads to the shift of the  $\tau_f$  value towards the side of negative values. There exists a phase transition from  $\text{L}_4\text{MS}$  to  $(\text{Li}_2\text{SnO}_3)_{ss}$  above  $1200^\circ\text{C}$ . That is to say, as the sintering temperature is higher  $1200^\circ\text{C}$ , the ceramic sample will be composed of  $(\text{Li}_2\text{SnO}_3)_{ss}$  and  $\text{L}_2\text{MS}(\text{MgO})_{ss}$  phases [23]. However, the relative content of  $(\text{Li}_2\text{SnO}_3)_{ss}$  and  $\text{L}_2\text{MS}(\text{MgO})_{ss}$  phases seems insensitive to the rise of sintering temperature, which also fits well to the phase diagram of  $\text{Li}_2\text{SnO}_3$  and  $\text{MgO}$ . Considering that pure  $\text{Li}_2\text{SnO}_3$  ceramics possess microwave dielectric properties of  $\epsilon_r = 11.4$ ,  $\tau_f = 14 \text{ ppm/}^\circ\text{C}$  and relatively low  $Q_{xf} = 13,100 \text{ GHz}$  [24], it may help deteriorate the  $Q_{xf}$  values of the composite ceramic. Owing to large negative values of  $\tau_f$  for  $\text{L}_2\text{MS}$ , the composite sample sintered at temperatures higher than  $1200^\circ\text{C}$  remains a relatively large negative value of  $\tau_f$ .

For the purpose of reducing sintering temperature and further suppressing the phase transition from  $\text{L}_4\text{MS}$  to  $\text{Li}_2\text{SnO}_3$ , 3–10 wt% LiF was added into the samples as sintering aids. The apparent density and  $\epsilon_r$  of  $\text{LSM}_{1/6}\text{O}$ -y wt.% LiF ceramics sintered at various temperatures are shown in **Fig. 2**. As sintering temperature increases, the apparent densities of all compositions firstly increase to their respective maximum values approximately at  $1000^\circ\text{C}$

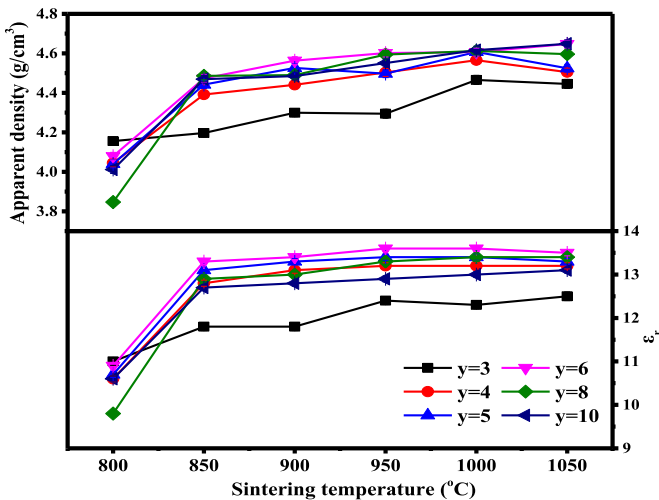


**Fig. 2.** Apparent density and  $\epsilon_r$  for  $\text{LSM}_{1/6}\text{O}-y$  wt.% LiF ceramics sintered at different temperatures.

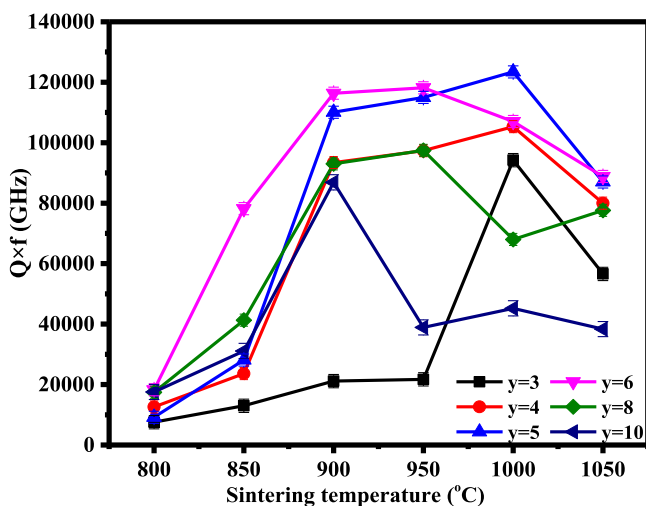
and then decreases with further increasing sintering temperature. For the same composition, the variation of  $\epsilon_r$  with changing sintering temperature presents a tendency similar to that of the apparent density. This result indicates that the sample density should be a dominant factor influencing permittivity. At the same sintering temperature, the difference in permittivity for different compositions should be mainly attributed to the sample density and the content of glass phase owing to the addition of sintering aid LiF. As a result, a relatively low  $\epsilon_r$  can be achieved approximately at  $y = 3$  and  $y = 10$ . Nevertheless, for samples with  $y = 5$  and  $y = 6$ , the sample density and  $\epsilon_r$  keep almost constant in the sintering temperature range of  $850\text{ }^\circ\text{C}$ – $1050\text{ }^\circ\text{C}$ , indicating that these two samples have been well densified within the above temperature range.

Fig. 3 illustrates the Qxf value of  $\text{LSM}_{1/6}\text{O}-y$  wt.% LiF ceramics sintered at different temperatures. It can be seen that the Qxf values of each composition firstly increase with increasing sintering temperature, then reach the maximum values, and decrease finally with further increasing temperature. The improvement in Qxf

values of each composition from  $800\text{ }^\circ\text{C}$  to  $950\text{ }^\circ\text{C}$  should be mainly attributed to the increase of sample density. A rapid deterioration of Qxf values from  $1000\text{ }^\circ\text{C}$  to  $1050\text{ }^\circ\text{C}$  may be due to the evaporation of lithium at higher temperatures. The optimal properties shift slightly towards the low temperature as the content of LiF increases. In addition, a higher content of sintering aid LiF might cause the formation of more glass phases in the sample at room temperature after sintering. The SEM images of  $\text{LSM}_{1/6}\text{O}-y$  wt.% LiF ( $y = 5, 6$ ) ceramics sintered at  $850\text{ }^\circ\text{C}$  and  $1000\text{ }^\circ\text{C}$  are displayed in Fig. 4. It can be seen that these samples have been well densified, indicating LiF doping significantly promotes the sintering behavior. Moreover, the grain size does not distinctly change with sintering temperature. However, as shown in Fig. 4(c), excessive LiF liquid phase (as indicated by arrows) in the  $y = 6$  sample can be observed near the grain boundary, as compared with the  $y = 5$  sample shown in Fig. 4(b), which would produce negative impacts on Qxf values. Nevertheless, excellent microwave dielectric properties of  $\epsilon_r = 13.4$ ,  $\text{Qxf} = 123,440\text{ GHz}$  (@  $9.68\text{ GHz}$ ) and  $\tau_f = -4.3\text{ ppm}/^\circ\text{C}$  were obtained in the  $y = 5$  sample sintered at  $1000\text{ }^\circ\text{C}$ .

The  $\tau_f$  values of  $\text{LSM}_{1/6}\text{O}-y$  wt.% ceramics samples with  $y = 5$  and  $y = 6$  sintered at different sintering temperatures are shown in Fig. 5. It can be seen that the  $\tau_f$  values slightly change from  $-9\text{ ppm}/^\circ\text{C}$  to  $-3\text{ ppm}/^\circ\text{C}$  with increasing sintering temperature from  $850\text{ }^\circ\text{C}$  to  $1050\text{ }^\circ\text{C}$  probably due to the variation of the phase content. Normalized XRD patterns of  $\text{LSM}_{1/6}\text{O}-6$  wt.% LiF ceramics sintered at  $800\text{ }^\circ\text{C}$ – $1050\text{ }^\circ\text{C}$  for 6 h are displayed in Fig. 6. All diffraction peaks can be well indexed according to the  $\text{L}_4\text{MS}$  and  $\text{L}_2\text{MS}(\text{MgO})_{ss}$  phases (JCPDS #37-1164 and JCPDS #39-0932) and no any other phases can be observed. The intensity of three major diffraction peaks near  $36^\circ$ ,  $42^\circ$  and  $62^\circ$  for the  $\text{L}_2\text{MS}(\text{MgO})_{ss}$  phase apparently increases with increasing sintering temperature from  $800\text{ }^\circ\text{C}$  to  $1050\text{ }^\circ\text{C}$ , indicating that the relative content of  $\text{L}_2\text{MS}(\text{MgO})_{ss}$  phase increases. Although the relative content of  $\text{L}_4\text{MS}$  and  $\text{L}_2\text{MS}(\text{MgO})_{ss}$  phases in both samples varies slightly with changing sintering temperature, the  $y = 5$  and  $y = 6$  samples do not show big differences in  $\tau_f$  values with changing sintering temperature. This is probably because the  $\tau_f$  values of  $\text{L}_2\text{MS}(\text{MgO})_{ss}$  and  $\text{L}_4\text{MS}$  phases are close in absolute values, so that the  $\tau_f$  values of the as-sintered composite ceramic is not very sensitive to their phase contents. For LTCC applications, desirable microwave dielectric properties of  $\epsilon_r = 13.0$ ,  $\text{Qxf} = 78,180\text{ GHz}$  and  $\tau_f = -9\text{ ppm}/^\circ\text{C}$  can be achieved in the composite sample with  $y = 6$  sintered at  $850\text{ }^\circ\text{C}$ . In spite of Li-containing compositions in current study, it is noteworthy that they are not sensitive to the humidity since all the samples were placed in air for a few days before the property measurement.

Table 1 presents a comparison of microwave dielectric ceramics for a few Li-based composite ceramics for LTCC applications. It can be seen that the  $\text{LSM}_{1/6}\text{O}-6$  wt.% LiF ceramic in current study exhibits larger application potentials because of much higher Qxf values. To evaluate chemical compatibility with silver, the composite ceramic powder was co-fired with 30 wt% Ag powder at  $850\text{ }^\circ\text{C}$  for 6 h. As shown in Fig. 7, all diffraction peaks of the co-fired sample can be well indexed to the  $\text{L}_4\text{MS}$ ,  $\text{L}_2\text{MS}(\text{MgO})_{ss}$  and Ag, indicating that no any chemical reaction occurs between the composite ceramic and the Ag particle. This could be further confirmed by the SEM image of the co-fired sample, as shown in the inset of Fig. 7. A distinct boundary between the ceramic grains and Ag particles can be observed, indicating silver particles can stably exist in the composite ceramic during sintering. Therefore, the self-composite ceramic of  $\text{L}_4\text{MS}$  and  $\text{L}_2\text{MS}(\text{MgO})_{ss}$  phases reported in this work possesses not only a good chemical compatibility with Ag electrode but also excellent microwave dielectric properties, being expected as a promising candidate material for LTCC applications.



**Fig. 3.** Qxf values of  $\text{LSM}_{1/6}\text{O}-y$  wt.% LiF ceramics sintered at different temperatures.

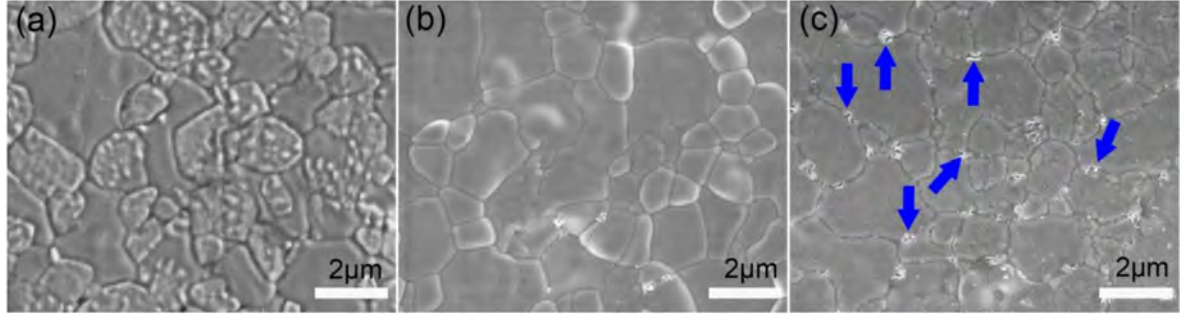


**Fig. 4.** SEM images of  $\text{LSM}_{1/6}\text{O}-y$  wt.% LiF ceramics sintered at various temperatures: (a)  $y = 6$ , at  $850\text{ }^\circ\text{C}$  (b)  $y = 5$ , at  $1000\text{ }^\circ\text{C}$  (c)  $y = 6$ , at  $1000\text{ }^\circ\text{C}$ .

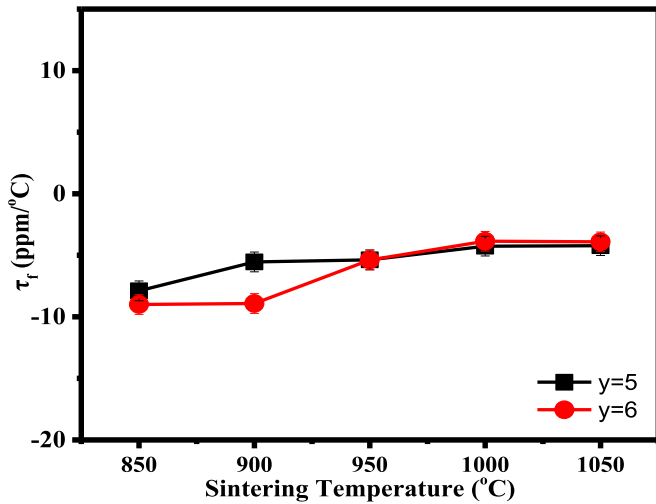


**Fig. 5.** The  $\tau_f$  values of  $\text{LSM}_{1/6}\text{O}-y$  wt.% LiF ( $y = 5-6$ ) ceramics sintered at different temperatures.

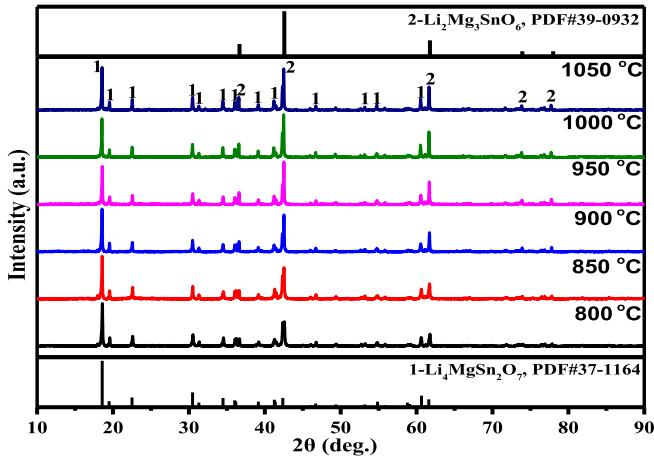


**Fig. 6.** XRD patterns of  $\text{LSM}_{1/6}\text{O}-6$  wt.% LiF ceramics sintered at different temperatures for 6 h.

#### 4. Conclusions

In present work, the phase evolution, sintering behavior and microwave dielectric properties of the  $\text{LSM}_{1/6}\text{O}-y$  wt.% LiF self-composite ceramics have been investigated in detail. The XRD results reveal that  $\text{L}_4\text{MS}$  phase tends to decompose into the  $\text{Li}_2\text{SnO}_3$

**Table 1**

Comparison of microwave dielectric properties for a few Li-based composite ceramics for LTCC applications.

| Compounds  | S.T. ( $^\circ\text{C}$ ) | $\epsilon_r$ | $Q \times f$ (GHz) | $\tau_f$ (ppm/ $^\circ\text{C}$ ) | Ref.      |
|--|---------------------------|--------------|--------------------|-----------------------------------|-----------|
| $0.86\text{Li}_2\text{TiO}_3\text{-}0.14\text{Li}_2\text{CeO}_3$   | 850                       | 21.2         | 59,310             | -7.4                              | [6]       |
| $\text{Li}_2\text{MgTiO}_4\text{-}10$ wt.% LiF<br>-12 wt.% $\text{Ca}_{0.8}\text{Sr}_{0.2}\text{TiO}_3$              | 900                       | 18           | 34,800             | 4                                 | [19]      |
| $\text{Li}_2\text{ZnTi}_3\text{O}_8\text{-}4$ wt.% $\text{TiO}_2$<br>-1 wt.% $\text{CaO-B}_2\text{O}_3\text{-SiO}_2$ | 900                       | 26.9         | 23,560             | -1.5                              | [25]      |
| $\text{Li}_2\text{MgTi}_3\text{O}_8\text{-}0.5$ wt% BCB  | 900                       | 26           | 36,200             | -2                                | [26]      |
| $\text{LSM}_{1/6}\text{O}-6$ wt.% LiF  | 850                       | 13.0         | 78,180             | -9                                | This work |

S.T. Sintering temperature.

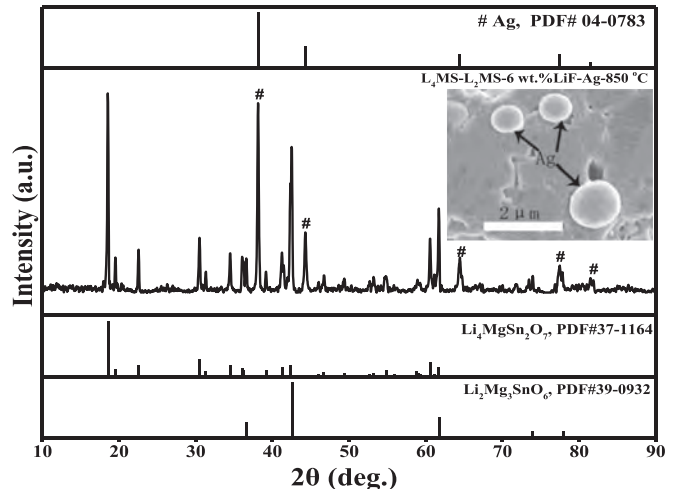


**Fig. 7.** XRD pattern and SEM image of the  $\text{LSM}_{1/6}\text{O}-6$  wt.% LiF sample co-fired with Ag at  $850\text{ }^\circ\text{C}$  for 6 h.

phase as sintered above  $1200\text{ }^\circ\text{C}$ . Doping LiF sintering aid can not only reduce the sintering temperature to suppress the decomposition of  $\text{L}_4\text{MS}$  phase at high temperature, but also help achieve dense ceramic samples. The relative content of  $\text{L}_2\text{MS}((\text{MgO})_{ss})$  and  $\text{L}_4\text{MS}$  phases prove to increase with changing sintering temperature, keeping good consistency with the XRD data and the phase diagram. Excellent microwave dielectric properties of  $\epsilon_r = 13.4$ ,  $Qxf = 123,440$  GHz and  $\tau_f = -4.3$  ppm/ $^\circ\text{C}$  were obtained in the sample with  $y = 5$  sintered at  $1000\text{ }^\circ\text{C}$ . Besides, a high  $Qxf$  value of 78,180 GHz and near-zero  $\tau_f$  of  $-9$  ppm/ $^\circ\text{C}$  could be achieved in the sample with  $y = 6$  sintered at  $850\text{ }^\circ\text{C}$ , together with a good chemical compatibility with Ag, indicating its large potential for LTCC applications.

## Declaration of competing interest

The authors declare that they have no known competing financial interests or personal relationships that could have appeared to influence the work reported in this paper.

## CRediT authorship contribution statement

**Shuang Zhang:** Writing - original draft. **Ruzhong Zuo:** Supervision.

## Acknowledgments

Financial support from the Anhui Provincial Natural Science Foundation (1508085JGD04) is gratefully acknowledged.

## References

- [1] M.T. Sebastian, H. Jantunen, Low loss dielectric materials for LTCC applications: a review, *Int. Mater. Rev.* 53 (2008) 57–90.
- [2] D. Zhou, L.X. Pang, D.W. Wang, C. Li, B.B. Jin, I.M. Reaney, High permittivity and low loss microwave dielectrics suitable for 5G resonators and low temperature co-fired ceramic architecture, *J. Mater. Chem. C* 5 (2017) 10094–10098.
- [3] M. Valant, D. Suvorov, Chemical compatibility between silver electrodes and low-firing binary-oxide compounds: conceptual study, *J. Am. Ceram. Soc.* 83 (2000) 2721–2729.
- [4] D. Zou, Q.L. Zhang, H. Yang, S.C. Li, Low temperature sintering and microwave dielectric properties of  $\text{Ba}_2\text{Ti}_3\text{Nb}_4\text{O}_{18}$  ceramics for LTCC applications, *J. Eur. Ceram. Soc.* 28 (2008) 2777–2782.
- [5] J.J. Bian, J.Y. Wu, L. Wang, Structural evolution, sintering behavior and microwave dielectric properties of  $(1-x)\text{Li}_3\text{NbO}_4-x\text{LiF}$  ( $0 \leq x \leq 0.9$ ), *J. Eur. Ceram. Soc.* 32 (2012) 1251–1259.
- [6] W.Q. Liu, R.Z. Zuo, A novel  $\text{Li}_2\text{TiO}_3$ - $\text{Li}_2\text{CeO}_3$  ceramic composite with excellent microwave dielectric properties for low-temperature cofired ceramic applications, *J. Eur. Ceram. Soc.* 38 (2018) 119–123.
- [7] D. Zhou, H. Wang, L.X. Pang, X. Yao, X.G. Wu, Microwave dielectric characterization of a  $\text{Li}_3\text{NbO}_4$  ceramic and its chemical compatibility with silver, *J. Am. Ceram. Soc.* 91 (2008) 4115–4117.
- [8] H.H. Guo, D. Zhou, L.X. Pang, Z.M. Qi, Microwave dielectric properties of low firing temperature stable scheelite structured  $(\text{Ca},\text{Bi})(\text{Mo},\text{V})\text{O}_4$  solid solution ceramics for LTCC applications, *J. Eur. Ceram. Soc.* 39 (2019) 2365–2373.
- [9] L.X. Pang, D. Zhou, D.W. Wang, J.X. Zhao, W.G. Liu, Z.X. Yue, I.M. Reaney, Temperature stable  $K_{0.5}(\text{Nd}_{1-x}\text{Bi}_x)_{0.5}\text{MoO}_4$  microwave dielectrics ceramics with ultra-low sintering temperature, *J. Am. Ceram. Soc.* 101 (2018) 1806–1810.
- [10] Z.F. Fu, P. Liu, J.L. Ma, X.G. Zhao, H.W. Zhang, Novel series of ultra-low loss microwave dielectric ceramics:  $\text{Li}_2\text{Mg}_3\text{BO}_6$  ( $B = \text{Ti}, \text{Sn}, \text{Zr}$ ), *J. Eur. Ceram. Soc.* 36 (2016) 625–629.
- [11] J.L. Ma, Z.F. Fu, P. Liu, Y. Liu, Novel temperature stable  $\text{Li}_2\text{Mg}_3\text{TiO}_6-\text{SrTiO}_3$  composite ceramics with high Q for LTCC applications, *Mater. Chem. Phys.* 200 (2017) 264–269.
- [12] J. Zhang, R.Z. Zuo, J. Song, Y.D. Xu, M. Shi, Low-loss and low-temperature firable  $\text{Li}_2\text{Mg}_3\text{SnO}_6-\text{Ba}_3(\text{VO}_4)_2$  microwave dielectric ceramics for LTCC applications, *Ceram. Int.* 44 (2018) 2606–2610.
- [13] H.T. Wu, E.S. Kim, Correlations between crystal structure and dielectric properties of high-Q materials in rock-salt structure  $\text{Li}_2\text{O}-\text{MgO}-\text{BO}_2$  ( $B = \text{Ti}, \text{Sn}, \text{Zr}$ ) systems at microwave frequency, *RSC Adv.* 6 (2016) 47443–47453.
- [14] J. Song, J. Zhang, R.Z. Zuo, Ultrahigh Q values and atmosphere-controlled sintering of  $\text{Li}_{2(1+x)}\text{Mg}_3\text{ZrO}_6$  microwave dielectric ceramics, *Ceram. Int.* 43 (2017) 2246–2251.
- [15] Z.X. Fang, B. Tang, F. Si, E.Z. Li, H.Y. Yang, S.R. Zhang, Phase Evolution, structure and microwave dielectric properties of  $\text{Li}_{2+x}\text{Mg}_3\text{SnO}_6$  ( $x = 0.00–0.12$ ) ceramics, *Ceram. Int.* 43 (2017) 13645–13652.
- [16] J.J. Bian, Y.F. Dong, Sintering behavior, microstructure and microwave dielectric properties of  $\text{Li}_{2+x}\text{TiO}_3$  ( $0 \leq x \leq 0.2$ ), *Mater. Sci. Eng. B* 176 (2011) 147–151.
- [17] R.Z. Zuo, J. Zhang, J. Song, Y.D. Xu, Liquid-phase sintering, microstructural evolution, and microwave dielectric properties of  $\text{Li}_2\text{Mg}_3\text{SnO}_6$ - $\text{LiF}$  ceramics, *J. Am. Ceram. Soc.* 101 (2018) 569–576.
- [18] Y.X. Mao, H.L. Pan, Y.W. Zhang, Q.Q. Liu, H.T. Wu, Effects of LiF addition on the sintering behavior and microwave dielectric properties of  $\text{Li}_2\text{Mg}_3\text{SnO}_6$  ceramics, *J. Mater. Sci. Mater. Electron.* 28 (2017) 13278–13282.
- [19] C.J. Pei, G.G. Yao, P. Liu, J.P. Zhou, Low temperature sintering and microwave dielectric properties of  $\text{Li}_2\text{MgTiO}_4$ -based temperature stable ceramics, *Mater. Lett.* 184 (2016) 57–59.
- [20] Z.F. Fu, P. Liu, J.L. Ma, B.C. Guo, X.M. Chen, H.W. Zhang, Microwave dielectric properties of low-fired  $\text{Li}_2\text{SnO}_3$  ceramics co-doped with  $\text{MgO}$ - $\text{LiF}$ , *Mater. Res. Bull.* 77 (2016) 78–83.
- [21] R.Z. Zuo, H. Qi, F. Qin, Q.L. Dai, A new Li-based ceramic of  $\text{Li}_4\text{MgSn}_2\text{O}_7$ : synthesis, phase evolution and microwave dielectric properties, *J. Eur. Ceram. Soc.* 38 (2018) 5442–5447.
- [22] M. Castellanos, A.R. West, Compound and solid solution formation in the system,  $\text{Li}_2\text{SnO}_3$ - $\text{MgO}$ , *J. Mater. Sci. Lett.* 3 (1984) 786–788.
- [23] Z.X. Fang, B. Tang, Y. Yuan, X. Zhang, S.R. Zhang, Structure and microwave dielectric properties of the  $\text{Li}_{2/3(1-x)}\text{Sn}_{1/3(1-x)}\text{Mg}_x\text{O}$  systems ( $x = 0–4/7$ ), *J. Am. Ceram. Soc.* 101 (2018) 252–264.
- [24] Y.N. Wang, Y.C. Chen, R.Y. Syu, Effect of sintering temperature on microstructures and microwave dielectric properties of  $\text{Li}_2\text{SnO}_3$  ceramics, *J. Mater. Sci. Mater. Electron.* 26 (2015) 1494–1499.
- [25] Y.X. Li, J.S. Li, B. Tang, S.R. Zhang, H. Li, Z.J. Qin, H.T. Chen, H. Yang, H. Tu, Low temperature sintering and dielectric properties of  $\text{Li}_2\text{ZnTi}_3\text{O}_8$ - $\text{TiO}_2$  composite ceramics doped with  $\text{CaO}$ - $\text{B}_2\text{O}_3$ - $\text{SiO}_2$  glass, *J. Mater. Sci. Mater. Electron.* 25 (2014) 2780–2785.
- [26] X.L. Chen, H.F. Zhou, L. Fang, X.B. Liu, Y.L. Wang, Microwave dielectric properties and its compatibility with silver electrode of  $\text{Li}_2\text{MgTi}_3\text{O}_8$  ceramics, *J. Alloys Compd.* 509 (2011) 5829–5832.